Figure 3. (a), (b) ^{129}Xe NMR spectrum of excess xenon on Linde 13X zeolite, obtained using 40 single pulses at 40-s repetition rate; lines due to solid, liquid, gaseous, and absorbed xenon are labeled s, l, g, and a respectively; (c), (d) ^{129}Xe NMR spectrum of xenon in hydrogen mordenite obtained using 400 single pulses at 4-s repetition rate.

symmetry axis.[7] The ends of the cages are formed by hexagonal rings consisting of six hydrogen-bonded OH units, the phenyl groups forming the cage walls. The ^{129}Xe line shape is characteristic of an axial shielding tensor with $\Delta\sigma = 160$ ppm so that the shielding along the cage axis is greater than that perpendicular to the axis. Figure 1c shows that on spinning the Xe–β-quinol sample at the magic angle at ~ 2.5 kHz, the powder pattern is reduced to a single line at the average shielding value, 222 ppm with respect to xenon gas at zero density, plus several spinning side bands.

Figure 2a, the ^{129}Xe spectrum obtained for xenon trapped in the phenol clathrate,[9] consists of three overlapping axially symmetric powder patterns. The spectrum obtained when the sample is spun at the magic angle is shown in Figure 2b; the average shielding and shielding anisotropies are summarized in Table I. There are two kinds of cages in the phenol clathrates, one similar in shape and size to the β-quinol cage and the other an elongated, axially symmetric cage of length ~ 15 Å and diameter 4.3 Å which can hold three xenon atoms, one next to each hexagonal $(OH)_6$ ring at the ends of the cage and one in between these two. The three lines can then be assigned as follows: The high field line, with shielding parameters similar to the β-quinol line, can be assigned to xenon in the small cages, the most intense middle line to the xenons in the large cage near the hexagonal rings, and the low field line to the central xenon in the large cage.

Figure 2c shows the ^{129}Xe NMR spectrum obtained for a structure I clathrate hydrate[10] containing ethylene oxide (EO) and xenon as guest molecules. The larger EO molecules occupy mainly the large cages; the xenon is distributed between the large and small cages. The low field line corresponds to xenon atoms in the small, nearly spherical structure I cages of $m3$ symmetry and 3.91-Å free diameter. The high field line can be assigned to xenon in the large cage, an oblate spheroid of $\overline{42}m$ symmetry and ~ 4.33-Å free diameter. In this case the shielding along the cage axis is less than the shielding perpendicular to the axis.

Figure 3a,b shows the Xe spectra of a dehydrated sample[11] of zeolite 13X containing excess xenon. Separate signals can be seen for liquid, solid, gaseous, and sorbed xenon. At 160 K the bulk xenon not trapped in the zeolite is frozen, and its NMR signal is shifted to low field of the sorbed xenon line. Since the total amount of xenon in the sample is known and the two lines are completely resolved (Figure 3a), the integrated line intensities can be used to calculate the zeolite cage occupancy. In this instance, there were found to be 10–11 xenon atoms per cage, assuming that all xenon atoms occupy only the zeolite supercages. Evidently sorbed xenon does not freeze at the bulk xenon melting point.

Above the melting point, the liquid line shifts to high field of the sorbed xenon line. This suggests that the sorbed xenon may be considered to be a liquid somewhat denser than bulk liquid xenon.

Figures 3c and 3d show spectra for xenon sorbed on a hydrogen mordenite sample.[12] At 240 K, two relatively broad lines are evident, ~ 62 ppm apart. The low field line can be assigned to xenon in the side pockets of the mordenite and the high field line to xenon in the main channel. Evidently at 240 K there is no exchange of the two types of xenon. The relatively large line widths suggest that within the two types of sites there is a further distribution. At 302 K only a single line is observable so that the xenon in the main channel and the side pockets are in a state of rapid exchange.

The Xe resonances reported here and for the condensed phases all occur to the low field of the infinitely dilute gas line. The shielding of the atom with respect to the bare nucleus has been estimated to be $\sigma = 5642$ ppm,[13] the degree of shielding being reduced by the effect of collisions and electron overlap with adjacent molecules.

The intensity information derived from Xe NMR spectra allows the measurement of the occupancy of inequivalent sites and should allow the testing and refining of guest–host potential functions. A detailed discussion of the potential functions for clathrate hydrates will be given elsewhere.[14] The measurements presented for the porous solids suggest that Xe NMR spectroscopy may be used to good advantage to study both the nature of porous crystals and the dynamics of Xe sorbed in such systems. Extensions to the study of phase transitions in surface layers and thin films are also indicated.

(12) An ammonium mordenite was prepared by ion exchange from commercial sodium mordenite (Strem Chemical Co.) This was then calcined at 500 °C in air to yield the hydrogen form.
(13) G. Malli and C. Froese, *Int. J. Quantum. Chem.*, **1**, 95 (1967).
(14) J. A. Ripmeester and D. W. Davidson, *J. Mol. Struct.*, **75**, 67 (1981). J. S. Tse and D. W. Davidson, *ACS Symp. Series*, in press.

Organophosphorus Compounds: The First Applications of Sulfuryl Chloride Fluoride SO₂FCl in Synthesis

Andrzej Łopusiński and Jan Michalski*

*Polish Academy of Sciences
Centre of Molecular and Macromolecular Studies
90-362 Lodz, Boczna 5, Poland*

Although sulfuryl chloride fluoride SO₂FCl (**1**) is readily available[1] and has been used as a solvent,[2] its chemistry is almost unexplored. Our previous work on the reaction between sulfuryl chloride and esters **2** (X = S)[3] suggested that **1** should be useful for converting compounds **2** and related systems into fluoridates RR'P(O)F (**3**) and fluorophosphoranes R₃PF₂ (**5**). We now report that the reaction between compounds ⫸P═X and sulfuryl chloride fluoride makes available a variety of fluorinated organophosphorus compounds, including new potential enzyme inhibitors.

The thione derivatives **2** (R, R' = alkyl or alkoxy, X = S) with sulfuryl chloride fluoride in methylene chloride for 30 min at −78

(1) Tullock, C. W.; Coffman, D. D. *J. Org. Chem.* **1960**, *25*, 2016.
(2) Olah, G. A.; Bruce, M. R. *J. Am. Chem. Soc.* **1979**, *101*, 4765. Olah, G. A.; Bruce, M. R.; Clouet, F. L. *J. Org. Chem.* **1981**, *46*, 438.
(3) Skowrońska, A.; Mikolajczak, J.; Michalski, J. *J. Am. Chem. Soc.* **1978**, *100*, 5386.
(4) ³¹P NMR spectroscopy with an external H₃PO₄ reference. Negative chemical shift values indicate absorption at higher fields than H₃PO₄. ¹⁹F NMR spectroscopy with internal CFCl₃ reference.
(5) The cis–trans geometry for 2-fluoro-2-oxo-4-methyl-1,3,2-dioxaphosphorinans (**7**) and the axial preference of fluorine at phosphorus was established by: Okruszek, A.; Stec, W. J. *Z. Naturforsch. B* **1976**, *31b*, 354.
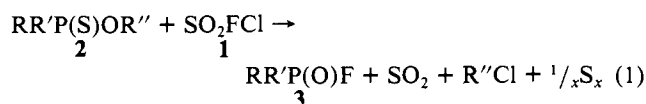(6) Schmutzler, R. *Angew. Chem.* **1965**, *77*, 530.

(9) M. Von Stackelberg, A. Hoverath, and C. Scheringer, *Z. Elektrochem.*, **62**, 123 (1958).
(10) D. W. Davidson in "Water, a Comprehensive Treatise", F. Franks, Ed., Plenum Press, New York, 1975.
(11) A commercial sample of Linde 13 X zeolite was dehydrated at 400 °C under vacuum.

°C afford the corresponding fluoridates **3** (80–90%) (reaction 1).

$$RR'P(S)OR'' + SO_2FCl \rightarrow$$
$$\quad\quad \mathbf{2} \quad\quad\quad \mathbf{1}$$
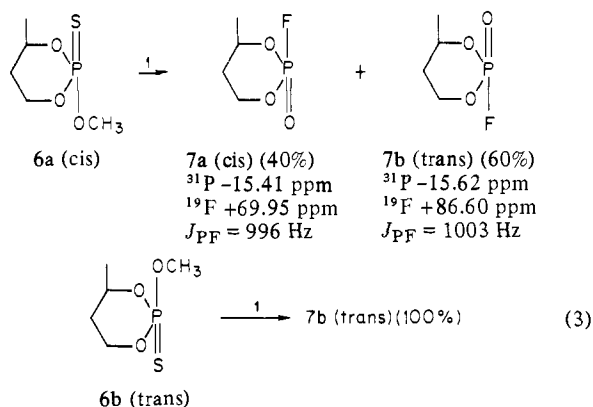$$RR'P(O)F + SO_2 + R''Cl + {}^1/_xS_x \quad (1)$$
$$\mathbf{3}$$

The phosphine sulfides **4** are distinctly less reactive but on prolonged warming at 20 °C were pressure with **1** yield the difluorophosphoranes **5** in satisfactory yields (reaction 2).
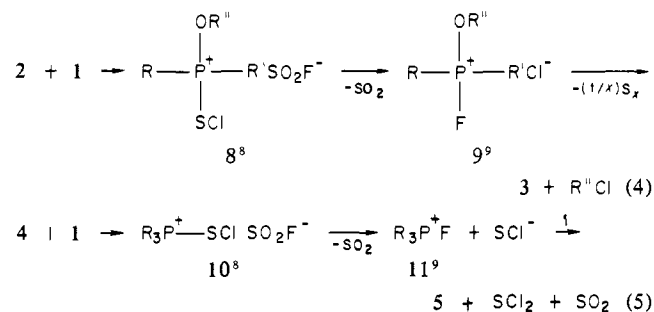
$$R_3P{=}S + 21 \rightarrow R_3PF_2 + 2SO_2 + SCl_2 \quad (2)$$
$$\mathbf{4} \quad\quad\quad \mathbf{5}$$
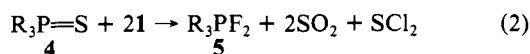
A single distillation or crystallization gave the pure fluorinated organophosphorus compounds (**3** and **5**),[7] which were characterized by ${}^{31}P$ and ${}^{19}F$ NMR spectroscopy, elemental analysis, and spectral comparisons with literature data.

Diastereoisomeric *cis*- (**6a**) and *trans*-2-methoxy-2-thioxo-4-methyl-1,3,2-dioxaphosphorinan (**6b**) are fluorinated stereoselectively by **1** (reaction 3).[5]

6a (cis)	7a (cis) (40%)	7b (trans) (60%)
	${}^{31}P$ −15.41 ppm	${}^{31}P$ −15.62 ppm
	${}^{19}F$ +69.95 ppm	${}^{19}F$ +86.60 ppm
	J_{PF} = 996 Hz	J_{PF} = 1003 Hz

$$\text{6b (trans)} \xrightarrow{\;1\;} \text{7b (trans)(100\%)} \quad (3)$$

The selenoesters **2** (R,R' = alkyl or alkoxy, X = Se) with sulfuryl chloride fluoride, under similar conditions as described for **2** (X = S), also give the corresponding fluorinated organophosphorus compounds **3** in excellent yields. The selenides **4** (X = Se) are distinctly more reactive than the corresponding sulfides and react vigorously below 0 °C. This provides, in our opinion, the simplest known synthesis of difluorophosphoranes **5** in 75–90% yields.[6]

The above experimental results, together with our previous studies on the chlorination of **2** (X = S),[3] indicated th mechanisms of reactions 4 and 5. The key step in each case is displacement of an SCl ligand by a strongly P-nucleophilic fluoride anion.

$$\mathbf{8}^8 \quad\quad\quad \mathbf{9}^9$$
$$\rightarrow 3 + R''Cl \quad (4)$$

$$4 + 1 \rightarrow R_3\overset{+}{P}{-}SCl \; SO_2F^- \xrightarrow{-SO_2} R_3\overset{+}{P}F + SCl^- \xrightarrow{1}$$
$$\mathbf{10}^8 \quad\quad\quad \mathbf{11}^9$$
$$5 + SCl_2 + SO_2 \quad (5)$$

Low-temperature FT ${}^{31}P$ NMR spectroscopy confirmed the presence of the intermediate phosphonium salts **8**, and **10** prior to ligand exchange.[8]

---

(7) NMR data for **3** (R ≡ R' ≡ C$_2$H$_5$O–): ${}^{31}P$ NMR −9.52 ppm, ${}^1J_{P-F}$ = 964 Hz; ${}^{19}F$ NMR 81.46 ppm. **3a** (R ≡ R' ≡ CH$_3$O–): ${}^{31}P$ NMR −7.9 ppm, ${}^1J_{P-F}$ = 974,1 Hz; ${}^{19}F$ NMR 80.6 ppm. **5** (R ≡ C$_6$H$_5$–): ${}^{31}P$ NMR −54.14 ppm, ${}^1J_{P-F}$ = 665.6 Hz; ${}^{19}F$ NMR −37.3 ppm.

(8) The ${}^{31}P$ spectral data of **8** and **10** are close to those observed in the reaction between **2** and **4** with sulfuryl chloride:[3] range of δ +40–+90.

(9) The structures of **9** and **11** need to be further confirmed by the independent synthesis.

Macrocyclic Effect in Transition-Metal Ion Complexes of a Mixed (Nitrogen, Oxygen) Donor Macrocycle

Robert D. Hancock* and Vivienne J. Thöm

Department of Chemistry, University of the Witwatersrand Johannesburg 2000, South Africa

Two types of evidence suggest that the macrocyclic effect is small or nonexistent when nitrogen donors are replaced by oxygens in complexes of macrocycles with transition-metal ions.[1] Firstly, the complexes of transition-metal ions such as Ag(I) with ligands such as 18-aneN$_2$O$_4$ demonstrate no extra stability compared with the open-chain analogue.[2] Secondly, Lindoy and co-workers[3] have studied the complexing abilities of ligands such as I and found them to be rather weak. Neither type is strong evidence that a normal macrocyclic effect cannot be obtained when nitrogens are replaced by oxygens. Ag(I) is not a typical transition-metal ion with its linear coordination geometry, and the "hole" in a ligand such as 18-aneN$_2$O$_4$ is too large for complexation to more typical transition-metal ions. Previous work[4] has shown the importance of inductive effects in stabilizing complexes of N-donor macrocycles so that the electron-withdrawing benzo groups on I are likely to be related to its poor complexing abilities. In order to study a mixed-donor macrocycle with appropriate geometry for coordination to transition-metal ions, and with no electron-withdrawing groups, 9-aneN$_2$O was synthesized by the route outlined in Figure 1. Ligand 9-aneN$_2$O may be compared with 9-aneN$_3$ to see what effect substituting an O for an N has on the complexing ability of the ligand and with HEEN and ODEN (Figure 2), which are its linear analogues. The important features of the macrocyclic effect in N-donor macrocycles are [4] (1) increased stability, (2) greater kinetic inertness, and (3) a more intense ligand field, compared with complexes of the linear analogue.

pK_1 and pK_2 were determined by standard potentiometric techniques[5] to be 9.59 and 5.32 for 9-aneN$_2$O. Log K values for 9-aneN$_2$O determined for Cu(II), Ni(II), and Zn(II) are shown in Table I, along with log K for 9-aneN$_3$, dien, HEEN, and ODEN. In Cu(II) the replacement of an N, which must occupy the unfavorable axial site in the 9-aneN$_3$ complex, has led to a more favorable macrocyclic effect in 9-aneN$_2$O, where the O presumably occupies the axial site. In Ni(II), log K_1 for 9-aneN$_2$O at 8.59 is larger than for any other diamine ligand. However, log K_1(9-aneN$_3$) − log K_1(dien) is 5.74, while log K_1(9-aneN$_2$O) − log K$_1$ (ODEN) is only 2.97 log units, a smaller macrocyclic effect. This could be evidence for the role of solvation[6] in producing the macrocyclic effect. Solvation of oxygen is weaker than nitrogen so that the desolvation that takes place when we cyclize ODEN to form 9-aneN$_2$O is less than when dien is cyclized to form 9-aneN$_3$. On the other hand, in Zn(II) the macrocyclic effect for 9-aneN$_2$O is 2.9 log units, similar to the 2.8 found for 9-aneN$_3$. This similarity would, as pointed out by a referee, militate against interpretation of the macrocyclic effect for Ni(II) with 9-aneN$_2$O and 9-aneN$_3$ in terms of desolvation effects.

Ligand 9-aneN$_2$O reacts with Zn(II) and Cu(II) fairly slowly, equilibrium taking about 20 min while Ni(II) takes several hours; 9-aneN$_3$ with Ni(II) takes several weeks.[7] Faster reaction makes 9-aneN$_2$O more convenient to study and may mean that mixed

(1) Melson, G. A. In "Coordination Chemistry of Macrocyclic Compounds"; Melson, G. A., Ed. Plenum Press: New York, 1979; pp 98–103. Lamb, J. D.; Izatt, R. M.; Christensen, J. J.; Eatough, D. J. *Ibid.*, pp 173–174.

(2) Frensdorff, H. K. *J. Am. Chem. Soc.* **1971**, *93*, 600–606. Anderegg, G. *Helv. Chim. Acta* **1975**, *58*, 1218–1225.

(3) Lindoy, L. F.; Lip, H. C.; Rea, J. H.; Smith, R. J.; Kim, H.; McPartlin, M.; Tasker, P. A. *Inorg. Chem.* **1980**, *19*, 3360–3365.

(4) Hancock, R. D.; McDougall, G. J. *J. Am. Chem. Soc.* **1980**, *102*, 6551–6553.

(5) Hancock, R. D.; Marsicano, F. *J. Chem. Soc., Dalton Trans.* **1978**, 228–234.

(6) Hinz, F. P.; Margerum, D. *Inorg. Chem.* **1974**, *13*, 2941–2949.

(7) Zompa, L. J. *Inorg. Chem.* **1978**, *17*, 2531–2536.

(8) Smith, R. M.; Martell, A. E. "Critical Stability Constants. Volume 2: Amines"; Plenum Press: New York, 1975.